Research Article | Vol. 25, No. 14 | 10 Jul 2017 | OPTICS EXPRESS 16002
Optics EXPRESS

Gaussian beam diffraction by two-dimensional refractive index modulation for high diffraction efficiency and large deflection angle

TIANSI WANG,[1] CHONG ZHANG,[2] ALEKSANDAR ALEKSOV,[3] ISLAM SALAMA,[2] AND ARAVINDA KAR[1,4]

[1]*CREOL, The College of Optics & Photonics, University of Central Florida, P.O. Box 162700, Orlando, FL 32816-2700, USA*
[2]*Intel - Assembly & Test Technology Development, 5000 W Chandler Blvd, Chandler, AZ 85226 USA*
[3]*Intel - Components research, 5000 W Chandler Blvd, Chandler, AZ 85226 USA*
[4]*Mechanical and Aeronautical Engineering and Material Science Engineering Department University of Central Florida, P.O. Box 162700, Orlando, FL 32816-2700, USA*
[*]*akar@creol.ucf.edu*

Abstract: The propagation of Gaussian beams is analyzed for an acousto-optic deflector by varying the refractive index in two-dimensions with a row of phased array piezoelectric transducers. Inhomogeneous domains of phase grating are produced by operating the transducers at different phase shifts, resulting in two-dimensional index modulation of periodic and sinc function profiles. Also different phase shifts provide a mechanism to steer the grating lobe in various directions and, therefore, the incident angle of the laser beam on the grating plane is automatically modified without moving the beam. Additionally, the acoustic frequency can be varied to achieve the Bragg condition for the new incident angle of the laser beam so that the diffraction efficiency of the deflector is maximized. The Gaussian beam is expressed in terms of planes and the second order coupled mode theory is implemented to analyze the diffraction of the beam. The diffraction efficiency is found to be nearly unity for optimal operating parameters of the acousto-optic device.

OCIS codes: (230.1950) Diffraction gratings; (230.1040) Acousto-optical devices.

References and links

1. G. R. B. E. Römer and P. Bechtold, "Electro-optic and acousto-optic laser beam scanners," Phys. Procedia **56**, 29–39 (2014).
2. G. J. Evans, P. A. Kirkby, K. M. Naga Srinivas Nadella, B. Marin, and R. Angus Silver, "Development and application of a ray-based model of light propagation through a spherical acousto-optic lens," Opt. Express **23**(18), 23493–23510 (2015).
3. J. Heberle, P. Bechtold, J. Strauß, and M. Schmidt, "Electro-optic and acousto-optic laser beam scanners," Laser-based Micro- and Nanoprocessing X, edited by Udo Klotzbach, Kunihiko Washio, Craig B. Arnold, Proc. of SPIE **9736**, 97360L–1:10 (2016).
4. N. J. Berg and J. M. Pellegrino, *Acousto-Optic Signal Processing* (Marcel Dekker, 1995), pp. 47–80.
5. G. Aubin, J. Sapriel, V. Ya. Molchanov, R. Gabet, P. Grosso, S. Gosselin, and Y. Jaouen, "Multichannel acousto-optic cells for fast optical crossconnect," Electron. Lett. **40**(7), 448–449 (2004).
6. S. N. Antonov and Yu. G. Rezvov, "Efficient multi-beam Bragg acoustooptic diffraction with phase optimization of a multifrequency acoustic wave," Tech. Phys. **52**(8), 1053–1060 (2007).
7. A. H. Mack, M. K. Trías, and S. G. J. Mochrie, "Precision optical trapping via a programmable direct-digital-synthesis-based controller for acousto-optic deflectors," Rev. Sci. Instrum. **80**, 016101 (2009).
8. Y. Kremer, J.-F. Léger, R. Lapole, N. Honnorat, Y. Candela, S. Dieudonné, and L. Bourdieu, "A spatio-temporally compensated acousto-optic scanner for two-photon microscopy providing large field of view," Opt. Express **16**(14), 10066–10076 (2008).
9. P. A. Kirkby, K. M. Srinivas Nadella, and R. A. Silver, "A compact acousto-optic lens for 2D and 3D femtosecond based 2-photon microscopy," Opt. Express **18**(13), 13720–13745 (2010).
10. M. G. Gazalet, M. Ravez, F. Haine, C. Bruneel, and E. Bridoux, "Acousto-optic low-frequency shifter," Appl. Opt. **33**(7), 1293–1298 (1994).

#291744 https://doi.org/10.1364/OE.25.016002
Journal © 2017 Received 30 Mar 2017; revised 2 Jun 2017; accepted 17 Jun 2017; published 28 Jun 2017

Optics EXPRESS

11. C. Grebing, S. Koke, and G. Steinmeyer, "Self-referencing of optical frequency combs, In: Conference on Lasers and Electro-Optics/International Quantum Electronics Conference." OSA Technical Digest, Optical Society of America, CTuK5 (2009).
12. M. R. Chatterjee, T.-C. Poon, and D. N. Sitter, Jr., "Transfer Function Formalism for Strong Acousto-Optic Bragg Diffraction of Light Beams with Arbitrary Profiles," Acta Acust. United Acust. **71**, 81–92 (1990).
13. D. Cao, P. P. Banerjee, and T.-C. Poon, "Image edge enhancement with two cascaded acousto-optic cells with contrapropagating sound," Appl. Opt. **37**(14), 3007–3014 (1998).
14. F. Almehmadi and M. R. Chatterjee, "Numerical examination of the nonlinear dynamics of a hybrid acousto-optic Bragg cell with positive feedback under profiled beam propagation," J. Opt. Soc. Am. B **31**(4), 833–841 (2014).
15. R. S. Chu and T. Tamir, "Diffraction of Gaussian beams by periodically modulated media for incidence close to a Bragg angle," J. Opt. Soc. Am. **66**(12), 1438–1440 (1976).
16. R. S. Chu, J. A. Kong, and T. Tamir, "Diffraction of Gaussian beams by a periodically modulated layer," J. Opt. Soc. Am. **67**(11), 1555–1561 (1977).
17. J. A. Kong, "Second-order coupled-mode equations for spatially periodic media," J. Opt. Soc. Am. **67**(6), 825–829 (1977).
18. M. G. Moharam, T. K. Gaylord, and R. Magnusson, "Bragg diffraction of finite beams by thick gratings," J. Opt. Soc. Am. **70**(3), 300–304 (1980).
19. S.-C. Wooh and Y. Shi, "Optimum beam steering of linear phased arrays," Wave Motion **29**(3), 245–265 (1999).
20. J. Aboujeib, A. Perennou, V. Quintard, and J. L. Bihan, "Planar phased-array transducers associated with specific electronic command for acoustooptic deflectors," J. Opt. A, Pure Appl. Opt. **9**(5), 463–469 (2007).
21. S. N. Antonov, A. V. Vainer, V. V. Proklov, and Y. G. Rezvov, "Extension of the angular scanning range of the acousto-optic deflector with a two-element phased-array piezoelectric transducer," Tech. Phys. **58**(9), 1346–1351 (2013).
22. J.-M. Andre, K. L. Guen, and P. Jonnard, "Rigorous coupled-wave theory for lossy volume grating in Laue geometry X-ray spectroscopy," submitted to J. Opt. Soc. Am. B (2014) <hal-01082017>, *https://hal.archives-ouvertes.fr/hal-01082017*.
23. T. Wang, C. Zhang, A. Aleksov, I. A. Salama, and A. Kar, "Dynamic two-dimensional refractive index modulation for high performance acousto-optic deflector," Opt. Express **23**(26), 33667–33680 (2015).
24. K. Nakahata and N. Kono, "3-D modeling of an ultrasonic phased array transducer and its radiation properties in solid," in *Ultrasonic Waves*, A. A. dos Santos, Jr., ed. (InTech, Croatia, 2012, ISBN: 978–953–51–0201–4), pp. 59–80.
25. T. Wang, C. Zhang, A. Aleksov, I. Salama, and A. Kar, "Two-dimensional analytic modeling of acoustic diffraction for ultrasonic beam steering by phased array transducers," Ultrasonics **76**, 35–43 (2017).
26. T.-S. Wang, C. Zhang, A. Aleksov, I. A. Salama, and A. Kar, "Effect of large deflection angle on the laser intensity profile produced by acousto-optic deflector scanners in high precision manufacturing," J. Laser Appl. **28**, 012012 (2016).
27. T. Wang, C. Zhang, A. Aleksov, I. Salama, and A. Kar, "Two-dimensional refractive index modulation by phased array transducers in acousto-optic deflectors," Appl. Opt. **56**(3), 688–694 (2017).
28. E. J. Galvez, *Gaussian Beams* (Colgate University, 2009).
29. M. Abramowitz and I. A. Stegun, Handbook of mathematical functions: with formulas, graphs, and mathematical tables (Courier Corporation, 1964), p. 885.
30. T. D. K. Ngoc and W. G. Mayer, "Numerical integration method for reflected beam profiles near Rayleigh angle," J. Acoust. Soc. Am. **67**(4), 1149–1152 (1980).
31. N. Uchida and N. Niizeki, "Acoustooptic deflection materials and techniques," Proc. IEEE **61**(8), 1073–1092 (1973).
32. R. S. Chu and T. Tamir, "Bragg diffraction of Gaussian beams by periodically modulated media," J. Opt. Soc. Am. **66**(3), 220–226 (1976).
33. W. R. Klein and B. D. Cook, "Unified Approach to Ultrasonic Light Diffraction," IEEE Trans. Sonics Ultrason. **14**(3), 123–134 (1967).

1. Introduction

Acousto-Optic Deflectors (AODs) are inertialess optical solid state devices to deflect and scan laser beams in numerous applications including microvia drilling in microelectronic industries for advanced high density packaging. Conventional mirror-based mechanical deflectors are prone to wear and tear, mechanical noise and drift due to moving parts such as rotating mirrors [1–3]. AODs are free of these drawbacks since they do not have any moving parts. Additionally, AODs allow higher deflection velocities, better accuracy in the scan angle and lower response time than the mechanical deflectors due to massless photons [1]. Various applications of AODs include optical communication [4–6], optical tweezers for molecule trapping [7], optical image scanners [8,9], and optical frequency shifters [10,11]. Two cascaded Bragg cells are generally used for two-dimensional scanning of lasers in imaging

Optics EXPRESS

applications. For improved image quality, the performance of acousto-optic diffraction gratings of one-dimensional refractive index modulation has been analyzed by spectral representation of the laser beam using Fourier transform [12–14].

Chu and Tamir [15] modeled the diffraction of Gaussian beams in dielectric media of periodically modulated permittivity by treating the incident beam as linear superposition of plane waves, and showed that both the refracted and Bragg-scattered beams split into two beams and this distortion lowers the diffraction efficiency compared to when a single plane wave is incident on the medium. Later they [15] applied the model to incident angles close to the Bragg angle and analyzed the effect of beam splitting by examining the major and minor lobe profiles for both the refracted and Bragg-scattered beams. Chu, Kong and Tamir [16] and Kong [17] presented a highly accurate second order coupled-mode model for the diffraction of Gaussian beams due to periodic modulation of permittivity, and showed that the conventional first order coupled-mode theory is accurate for small perturbation in the permittivity and that the second order approach must be used for strongly modulated media. In Ref [16], x-L should be read as x in Eqs. (25) and (26), and the exponential term should be $exp\left[ik_{3x}^{b}\left(x-L\right)+ik_{-1z}z\right]$ in Eq. (26). Moharam, Gaylord and Magnusson [18] modeled the diffraction of Gaussian beams in transparent volume gratings by two coupled first order partial differential equations based on a modified version of the two-dimensional coupled wave theory.

One-dimensional modulation of the refractive index, $n(z)$, has been considered in the above-mentioned studies. Also conventional AODs operate at small deflection angles, and high diffraction efficiency only over a narrow bandwidth of the acoustic frequency. However, advanced applications, such as high precision and high speed microvia drilling and image scanning, require large deflection angles for large-area processing and high diffraction efficiency over a wide acoustic bandwidth. Phased-array transducers have been incorporated to AODs for improving the deflection angle and bandwidth [19–21] by assuming one-dimensional index modulation that holds good for small tilting of the phase grating planes. Two-dimensional index modulation, $n(x,z)$, provides a mechanism to improve the performance of AODs further. Recently, Andre, Guen and Jonnard [22] applied a rigorous coupled-wave theory to lossy volume gratings with two-dimensional permittivity for X-ray spectroscopy and concluded that the rigorous approach, which is not based on the two-wave and the first derivative approximations, is necessary to accurately calculate the diffraction efficiency. Wang et al. [23] studied the effect of two-dimensional refractive index modulation on the diffraction of plane waves and showed that the deflection angle can be increased using phased array transducers and the diffraction efficiency is nearly unity over a wide acoustic bandwidth. The phase-shifted acoustic waves, which are emitted by the transducers, interfere inside the AOD to form a phase grating within which the refractive index varies in two dimensions. The grating lobe can be tilted to different angles by operating the transducers with appropriate time-delayed radio-frequency (RF) signals. This tilt in the grating automatically modifies the incident angle of the laser beam on the grating plane even though the laser is stationary [24]. So the frequency of the RF signal is changed to achieve the Bragg condition under this new angle of incidence, and thus the dynamic acousto-optic volume grating can improve the performance of AODs.

In this paper, the diffraction of Gaussian beams is studied for AODs of finite size with two-dimensional index modulation. Section 2 provides a summary of the AOD geometry and the index modulation used in this study. The Gaussian beam is represented by the superposition of plane waves and then the electric field is determined at the exit surface of the AOD using the plane wave solution from Ref [23]. The results and discussion are presented in Section 3 for TeO_2, and Ge-AODs based on the phase, frequency and amplitude modulations of the transducers for Ne-Ne and CO_2 lasers respectively.

Optics EXPRESS

2. Theoretical background

2.1 Two-dimensional refractive index modulation

AODs can be generally classified into two groups depending on whether a single transducer or phased-array transducers are used to operate the AODs. The drawbacks of single-transducer AODs are narrow acoustic bandwidth, small deflection angle and small scan angle. Phased-array transducers are utilized to overcome these shortcomings [6,23]. Phase-shifted acoustic waves, which are emitted by the transducers when they are operated with some time delays with respect to each other, propagate through the AOD medium as a tilted composite wavefront (Fig. 1) due to the diffraction and interference of the waves. Due to this acoustic effect, the atomic planes of the AOD medium are tilted as alternating compressed and rarefied layers with index modulation along the tilted planes. The composite wavefront can be steered in different directions by dynamically varying the time delays and, consequently, the index modulation planes can be tilted at various angles.

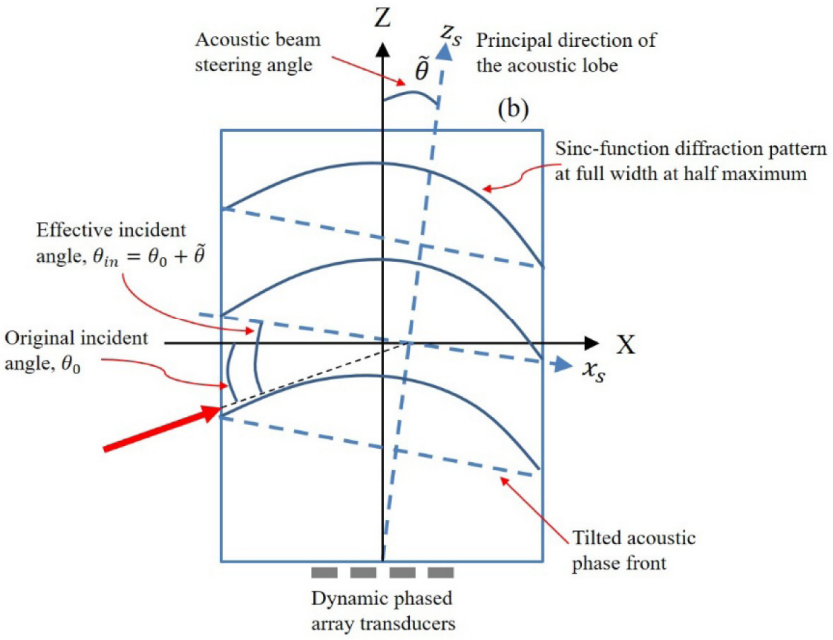

Fig. 1. Dynamic phased array transducers for acoustic beam steering to produce tilted phase fronts with a sinc-function diffraction pattern of the acoustic waves.

A typical steering angle, $\tilde{\theta}$, corresponding to the principal direction, z_s, of the acoustic diffraction lobe is presented in Fig. 1, showing that the new incident angle would be $\theta_{in} = \theta_0 + \tilde{\theta}$ for the tilted index modulation if the laser beam is originally incident on the unperturbed AOD at the angle θ_0. Using this acoustic beam steering mechanism, the angle of laser incidence on the tilted phase grating can be varied automatically without moving the original laser beam. For each steering angle, the frequency of the acoustic waves needs to be adjusted to ensure that θ_{in} corresponds to the Bragg angle of incidence for achieving large deflection angle given by θ_{in} and large diffraction efficiency given by the Bragg diffraction condition.

The above-mentioned acoustic effect also produces a two-dimensional phase grating in contrast to one-dimensional gratings in conventional AODs. The acoustic waves emitted by an array of transducers generally produces a diffraction pattern of the sinc-function shape in

Optics EXPRESS

Cartesian coordinates [25]. Since the variation of refractive index depends on the intensity distribution of the composite acoustic wavefront, the refractive index is considered to vary as a sinc-function in the transverse direction x_s in this study (Fig. 2). On the other hand, the refractive index varies periodically with the period Λ in the longitudinal direction z_s, where Λ is the wavelength of the acoustic waves in the AOD medium, and this periodic variation is taken as a cosine function. So the two-dimensional index profile in region II, $n_{II}(x_s, z_s)$, can be written as [26]:

$$n_{II}(x_s, z_s) = n_2(\lambda_0) + \Delta n \cos\left(\frac{2\pi}{\Lambda} z_s\right)\left(\frac{\sin(bx_s)}{bx_s}\right) \tag{1}$$

where $x_s = x\cos\tilde{\theta} - z\sin\tilde{\theta}$, $z_s = x\sin\tilde{\theta} + z\cos\tilde{\theta}$ and $\tilde{\theta}$ is the tilting angle.

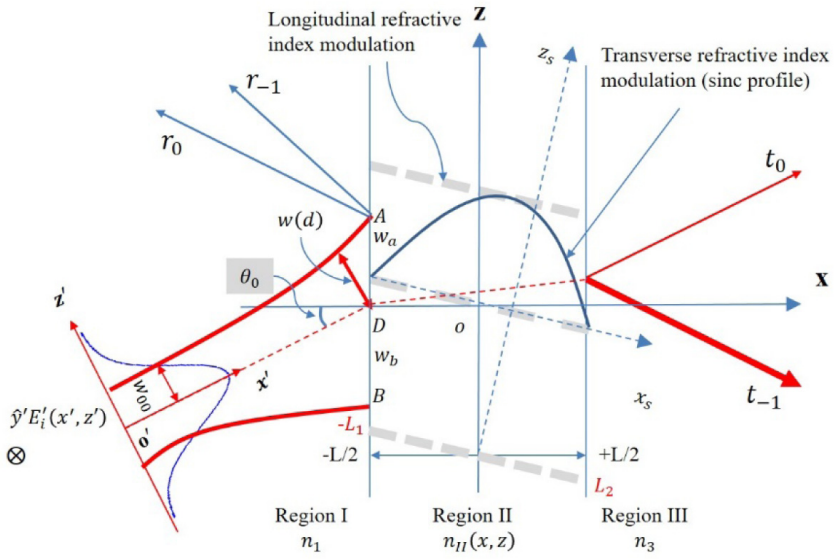

Fig. 2. Geometry for laser beam propagation in an AOD medium of two-dimensional refractive index variation caused by phased array transducers, $O'D$ = d.

where $n_2(\lambda_0)$ is the refractive index of the unperturbed acousto-optic medium at the wavelength of the incident light in vacuum, λ_0, and Δn is the maximum change in the refractive index that can be determined by considering the Acousto-optic effect [27]. The parameter b is a constant that defines the width of the central lobe of the sinc function. Since this function varies from a maximum value at the center of the lobe to zero at the edge of the lobe, the parameter b is so chosen that the index modulation is significant in the AOD medium. The central peak of the sinc function occurs at $x_s = 0$ and the lobe spans from $x_s = -L_1$ to $x_s = L_2$ (Fig. 2) to yield a significant index modulation. If L_m represents the larger of the two values L_1 and L_2, b can be determined by considering that L_m is the full width at half maximum of the sinc function, i.e.,

$$\frac{\sin(bL_m/2)}{bL_m/2} = \frac{1}{2} \tag{2}$$

The above-mentioned two-dimensional index $n_{II}(x_s, z_s)$ were used in the second order coupled-mode Maxwell equation by Wang et al. [23] to analyze the performance of AODs for

incident lights of plane wavefront. Their model is implemented in this paper for studying the diffraction of Gaussian beams by decomposing the beam into numerous plane waves.

2.2 Decomposition of Gaussian laser beam profiles into plane wave spectral components

The electric field of Gaussian laser beams can be written as follows [28]

$$E_i^{'}(x',z') = A_0 \frac{w_{00}}{w(x')} e^{-\left(\frac{z'}{w(x')}\right)^2} e^{ik_0 x'} e^{-i\phi(x')} e^{ik_0 \frac{z'^2}{2R(x')}} \tag{3}$$

in the Cartesian coordinate system (x',z') with the origin being at the center of the beam waist as shown in Fig. 2. Here A_0 is the peak electric field and w_{00} is the radius of the Gaussian beam waist which is located at the plane $x'=0$ The radius of the Gaussian beam at any other plane is given by $w(x') = w_{00}\sqrt{1+\left(x'/x_R^{'}\right)^2}$, $\phi(x')$ is the Gouy phase, $\phi(x') = \tan^{-1}\left(x'/x_R^{'}\right)$, $R(x')$ is the radius of curvature of the Gaussian laser wavefront, $R(x') = x' + x_R^{'2}/x'$, and $x_R^{'}$ is the Rayleigh range, $x_R^{'} = \pi w_{00}^2/\lambda_0$.

The laser beam is incident on the x = -L/2 surface of the AOD with the interception points A, D and B as shown in Fig. 2. The widths of the interception DA and DB are given by w_a and w_b respectively. These two widths are determined by applying the Gaussian beam radius $w(x')$ to the points A and B, which yield w_b and w_a that can be expressed as:

$$w_a = \frac{x_R^{'}\sqrt{\frac{\left(d^2 + x_R^{'2}\right)\cos^2\theta_0}{w_{00}^{\ 2}} - \sin^2\theta_0} + d\sin\theta_0}{\left(\frac{x_R^{'}\cos\theta_0}{w_{00}}\right)^2 - \sin^2\theta_0} \tag{4}$$

$$w_b = \frac{x_R^{'}\sqrt{\frac{\left(d^2 + x_R^{'2}\right)\cos^2\theta_0}{w_{00}^{\ 2}} - \sin^2\theta_0} - d\sin\theta_0}{\left(\frac{x_R^{'}\cos\theta_0}{w_{00}}\right)^2 - \sin^2\theta_0} \tag{5}$$

To analyze the laser beam propagation inside the AOD medium in the (x, z) coordinate system, the following coordinate transformation is applied to Eq. (3)

$$\begin{pmatrix} x' \\ z' \end{pmatrix} = \begin{pmatrix} (x+L/2)\cos\theta_0 + z\sin\theta_0 + d \\ -(x+L/2)\sin\theta_0 + z\cos\theta_0 \end{pmatrix} \tag{6}$$

to obtain the Gaussian beam profile as

$$E_i(x,z) = A(d)\, e^{-\left[\frac{-(x+L/2)\sin\theta_0 + z\cos\theta_0}{w(d)}\right]^2} e^{ik_0 \frac{\left[-(x+L/2)\sin\theta_0 + z\cos\theta_0\right]^2}{2R(d)}} e^{ik_0\left[(x+L/2)\cos\theta_0 + z.\sin\theta_0\right]} \tag{7}$$

where d is the distance from O' to D in Fig. 2, $A(d) = A_0 \frac{w_{00}}{w(d)} e^{ik_0 d} e^{-i\phi(d)}$ and θ_0 is the incident angle of the Gaussian beam; $w(d) = w_{00}\sqrt{1+d^2/x_R^{'2}}$ and $R(d) = d + x_R^{'2}/d$. The

Optics EXPRESS

electromagnetic field of the laser, $E_i(x,z)$, is expressed as a superposition of plane waves so that the solution of Ref [23], which was obtained for the diffraction of plane waves due to two-dimensional index modulation, can be implemented in this study.

2.3 Gaussian beam diffraction in AOD media with two-dimensional refractive index modulation

Fourier representation of $E_i(x,z)$ in terms of angular spectra provides a convenient way of expressing the electric field of an incident Gaussian beam as linear plane wave superposition, i.e.,

$$E_i(x,z) = \int_{-\infty}^{\infty} G(k_{0z}) \exp\left[i(k_{1x}x + k_{0z}z)\right] dk_{0z} \tag{8}$$

where $G(k_{0z})$ is the spectral amplitude and $\exp(ik_{1x}x)$ and $\exp(ik_{0z}z)$ are spectral components of wavenumbers k_{1x} and k_{oz} for the plane waves propagating in the x and z directions, respectively. $E_i(x,z)$ is incident on the incident surface of the AOD medium from region I ($x < -L/2$) with the wavenumber $k_1 = n_1 k_0$, where n_1 is the refractive index of medium I, $k_0 = 2\pi/\lambda_0$ and λ_0 is the wavelength of the incident laser in vacuum. So k_1, k_{1x} and k_{oz} can be related to each other by the expressions $k_{1x} = k_1\cos\theta$, $k_{0z} = k_1\sin\theta$ and $k_{1x} = \sqrt{k_1^2 - k_{0z}^2}$, where θ is the incident angle of an arbitrary plane wave of wavenumber k_1.

The unknown factor, i.e., the spectral amplitude $G(k_{0z})$, in Eq. (7) can be obtained by applying the Fourier inverse transform to Eq. (7) on the incident surface x = - L/2, which yields

$$G(k_{0z}) = \frac{1}{2\pi}\int_{-\infty}^{\infty} E_i(-L/2, z) e^{ik_{1x}L/2} e^{-ik_{0z}z} dz \tag{9}$$

In Fig. 2, $w(d)$ is the length scale for the 1/e-point of the electric field in $x'-z'$ coordinates. On the incident plane $x = -L/2$, however, the points A and B of distances $DA = w_a$ and $DB = w_b$ represent the 1/e-point of electric field. Since $w_a > w_b$, the length scale is taken as w_a.

$$E_i(-L/2, z) = A(d) e^{-\left(\frac{z\cos\theta_0}{w_a}\right)^2} e^{ik_0\frac{(z\cos\theta_0)^2}{2R(d)}} e^{ik_0\sin\theta_0 z} \tag{10}$$

Substituting Eq. (10) into Eq. (9), $G(k_{0z})$ is obtained as

$$G(k_{0z}) = \frac{A(d)}{2\pi}\sqrt{\frac{\pi}{\frac{1}{w_a^2} + ik_0\frac{\cos\theta_0}{2R(d)}}} e^{\frac{-(k_{0z}-k_0\sin\theta_0)^2}{4\left(\frac{1}{w_a^2}+ik_0\frac{\cos\theta_0}{2R(d)}\right)}} e^{ik_{1x}L/2} \tag{11}$$

As pointed out by Chu, Kong and Tamir [16], the transmitted beams in region III can be viewed as the linear superposition of plane wave solutions. Therefore, the electric field of the zeroth order beam in region III is

$$E_0(x,z) = \int_{-\infty}^{\infty} G(k_{0z}) t_0(k_{0z}) \exp\left(ik_{3,0x}x + ik_{0z}z\right) dk_{0z} \tag{12}$$

for $x \geq L/2$, and the Bragg-diffracted, i.e., −1 order, beam is

$$E_{-1}(x,z) = \int_{-\infty}^{\infty} G(k_{0z}) t_{-1}(k_{0z}) \exp\left(ik_{3,-1x}x + ik_{-1z}z\right) dk_{0z} \tag{13}$$

Optics EXPRESS

for $x \geq L/2$, where $t_0(k_{0z})$ and $t_{-1}(k_{0z})$ are the transmission coefficients for plane waves of wavenumber k_{0z} in the zeroth order and −1 order lights, respectively, at the exit surface x = L/2. Due to the propagation of acoustic waves of wavenumber K in the AOD medium, k_{0z} and k_{-1z} in Eqs. (12) and (13) are the z components of the zeroth and −1 order Floquet modes and are given by $k_{0z} = k_0 \sin\theta$ and $k_{-1z} = k_{0z} - K$. Similarly, $k_{3,0x}$ and $k_{3,-1x}$ are the x components of the zeroth and −1 order Floquet modes and are given by $k_{3,0x} = \sqrt{k_3^2 - k_{0z}^2}$ and $k_{3,-1x} = \sqrt{k_3^2 - k_{-1z}^2}$. Here $K = 2\pi/\Lambda$ and $k_3 = n_3 k_0$ where the wavelength of the acoustic waves in region II and the refractive index in region III are Λ and n_3, respectively. The transmission coefficients $t_0(k_{0z})$ and $t_{-1}(k_{0z})$ in Eqs. (12) and (13) are obtained for each plane wave component [23] by (i) applying the refractive index $n_{II}(x_s, z_s)$ into the Maxwell equation in region II, (ii) solving the coupled-mode Maxwell equations in regions I, II and III, and (iii) satisfying the boundary conditions at the interfaces of regions I and II, and II and III.

The integrations in Eqs. (12) and (13) are evaluated numerically using the extended trapezoidal rule [29]. To transform the limits of integration from the infinite range to a finite range, the limits on k_{0z} are considered as follows:

$$k_1 \sin\theta_0 - p\frac{2\pi}{w_a + w_b} \leq k_{0z} \leq k_1 \sin\theta_0 + p\frac{2\pi}{w_a + w_b} \tag{14}$$

where p is any positive number which is chosen to ensure that sufficient number of spectral components are selected for representing the Gaussian beam in terms of plane waves. Ngoc and Mayer [30] chose p = 1 for their studies on the intensity distribution of ultrasonic beams reflected from a liquid-solid interface. In the present study, p is found to be 5 to accurately represent the incident Gaussian laser beam as linear superposition of plane waves. The finite range of integration is discretized into M points with the interval $\Delta k_{0z} = \frac{4p\pi}{(w_a + w_b)(M-1)}$ and the value of the spectral component at any point m as $k_{0z,m} = k_{0z,1} + (m-1)\Delta k_{0z}$ for m = 1, 2,3, …, M where $k_{0z,1} = k_1 \sin\theta_0 - p\frac{2\pi}{w_a + w_b}$. Defining the integrands of Eqs. (12) and (13) at any point m as

$$E_{0,m} = \left[G(k_{0z})\, t_0(k_{0z}) \exp\left(ik_{3,0x}x + ik_{0z}z\right)\right]_{k_{0z}=k_{0z,m}} \tag{15}$$

$$E_{-1,m} = \left[G(k_{0z})\, t_{-1}(k_{0z}) \exp\left(ik_{3,-1x}x + ik_{-1z}z\right)\right]_{k_{0z}=k_{0z,m}} \tag{16}$$

the electric fields in the zeroth and −1 order modes can be approximately determined by the following expressions:

$$E_0(x,z) \approx \Delta k_{0z} \sum_{m=1}^{M} E_{0,m} - \frac{\Delta k_{0z}}{2}\left(E_{0,1} + E_{0,M}\right) \tag{17}$$

$$E_{-1}(x,z) \approx \Delta k_{0z} \sum_{m=1}^{M} E_{-1,m} - \frac{\Delta k_{0z}}{2}\left(E_{-1,1} + E_{-1,M}\right) \tag{18}$$

Equations (17) and (18) are used to analyze the performance of AODs for He-Ne and CO_2 lasers of wavelengths 632.8 nm 10.6 μm, respectively, and the corresponding AOD media are considered to be crystalline TeO_2 and Ge. The diffraction efficiency, which is defined as $\eta_D = |E_{-1}|^2 / |E_0|^2$, is determined numerically using Eqs. (17) and (18).

Optics EXPRESS

3. Results and discussion

To examine the transmitted behavior of the Gaussian beam diffracted by periodically modulated AO medium, several numerical calculations were carried out in this study based on the data listed in Table 1. The width of laser beam was w_{00} = 0.64 mm and the refractive indices in regions I and III were taken as $n_1 = n_3 = 1.0$. The accuracy of $E_0(x,z)$ and $E_{-1}(x,z)$ in Eqs. (17) and (18) depends on the choice of p and M. While p determines the range of spectral components chosen for plane wave decomposition of the Gaussian beam, M affects the convergence of the numerical integration by the extended trapezoidal rule. To verify the computational accuracy, the normalized intensity of the Gaussian beam is calculated by two approaches that are based on the exact expression of the input beam given by Eq. (7) and the spectral representation of the beam given by Eqs. (9) and (11). The results as obtained at the incident surface of the AOD medium with the beam waist on this surface, i.e., x = -L/2 and d = 0, as shown in Fig. 3 for the case of TeO_2 AOD. The two results were found to match well when p = 5 and M = 100, for both cases of TeO_2 and Ge AODs.

Table 1. Simulation parameters for TeO_2 and Ge crystals to deflect He-Ne and CO_2-lasers respectively [31].

AO material	Ge crystal	TeO_2 crystal
Density of AO medium, ρ [g/cm^3]	5.33	5.99
Laser wavelength, [μ m]	10.6 (CO_2 laser)	0.6328 (He-Ne laser)
Laser beam width, w_{00} [mm]	0.64	0.64
Refractive index, n_2	4.0	2.26
Acoustic speed for P-wave, [m/s]	5500	4200
Acoustic speed for S-wave, [m/s]	3510	616
Central acoustic frequency, [MHz]	70	75
Central acoustic wavelength, [μ m]	78.6	56

The results of this study are also compared to the beam profiles determined by Chu, Kong and Tamir [16] for one-dimensional index modulation, and their model is referred to as 1D-CKT model hereafter. For this comparison, the diffraction of the laser beam is simulated using Eqs. (17) and (18) for one-dimensional index modulation by setting the sinc function to unity in Eq. (1), and the laser beam profiles are obtained at the exit surface (x = L/2) as presented in Fig. 4. Although the profiles of both studies exhibit similar trend, the results do not match exactly and this discrepancy may be attributed to the method of solution. The transmission coefficients t_0 and t_{-1} in 1D-CKT model were based on Kong's [17] exact calculation for these two coefficients by solving an 8 × 8 matrix equation exactly. In the present study, the transmission coefficients were calculated by considering Wang's et al. [23] first order approximation of the electric field for each plane wave component of the Gaussian beam. The results, however, exhibit two dominant peaks in the −1 order diffracted beam showing non-Gaussian profiles and splitting of the beam. The zeroth order beam is also non-Gaussian with a fairly uniform irradiance profile showing distortion of the original Gaussian beam incident on the AOD.

Optics EXPRESS

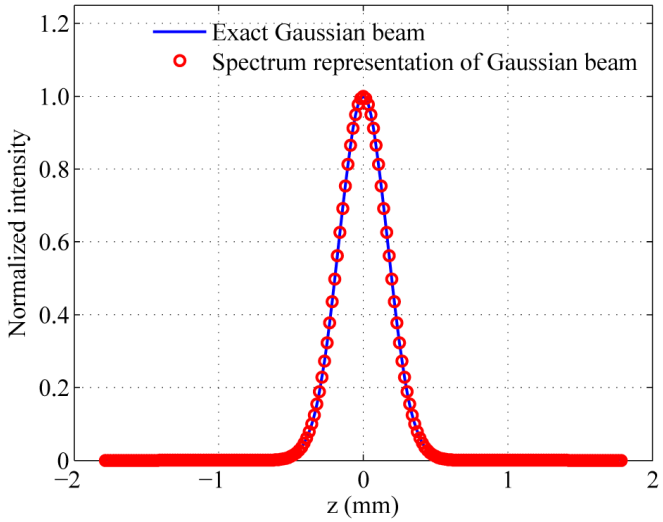

Fig. 3. Comparison between the plane wave superposition of a Gaussian beam and the exact Gaussian beam profile given by Eq. (7).

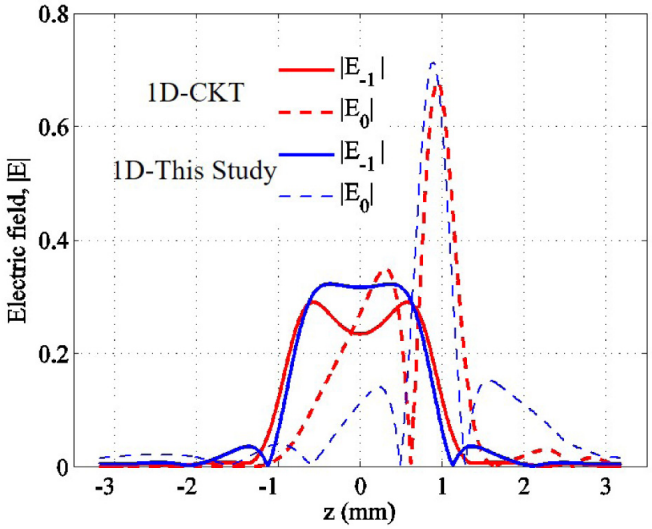

Fig. 4. Comparison of the Gaussian beam profiles at the exit surface of a TeO_2 AOD for one-dimensional refractive index modulation based on CKT 1-D model and the reduction of the current 2-D model to 1-D problem.

Optics EXPRESS

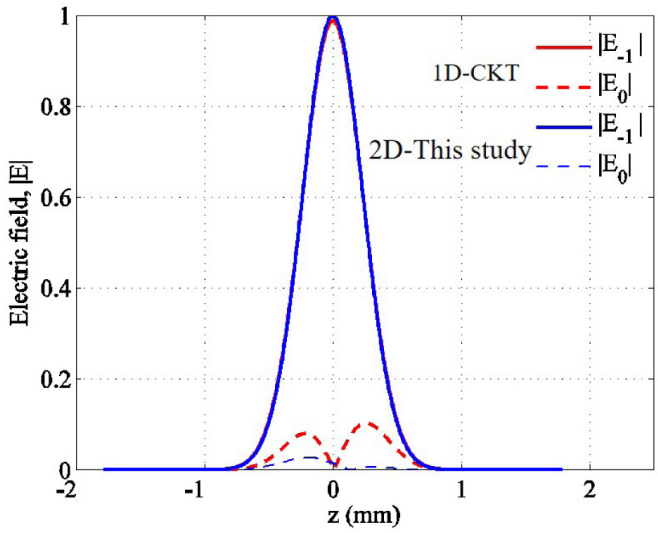

Fig. 5. Magnitude of the electric field (|E|) at the exit boundary for an AOD of thickness L, calculated using the Gaussian beam diffraction model of this study and the CKT model for F = 75 MHz, L = 2.24 cm and $\theta_{in} = 0.324^{o}$.

To examine the beam splitting and distortion, two-dimensional index modulation of this study, which is referred to as 2D model hereafter, is analyzed with optimized index modulation strength Δn as presented in Fig. 5. Results are obtained from both the 2D and 1D-CKT models for the optimized values of $\Delta n = 2.2 \times 10^{-5}$ and 1.4×10^{-5}, respectively, to achieve the maximum diffraction efficiency in each model. Both models yield Gaussian profile with beam splitting in the −1 order diffracted beam. The zeroth order beam, however, exhibits non-Gaussian profile with two peaks indicating beam splitting at the exit surface in Fig. 5. The beam distortion, which causes the beam splitting, occurs due to continuous exchange of energy between the zeroth and −1 order beams as they propagate through the AOD medium [32]. This continuous coupling of energy diffuses the energy over the entire irradiated region and, consequently, the beams are distorted to non-Gaussian profiles. For large distortions, the beams are sufficiently modified and each beam splits into two portions. The beam splitting is less dominant with much lower electric field in the 2D model than in the case of 1D-CKT model. Two-dimensional index modulation, therefore, allows more energy transfer to the −1 order beam than the one-dimensional index modulation and, consequently, higher diffraction efficiency can be achieved in the former case. Figure 6 examines the shape of the zeroth order split beam as it propagates in medium III away from the exit surface of the AOD medium. The zeroth order beam begins to separate from the −1 order beam for the AOD of thickness 2L in Fig. 6, but the profile of the zeroth order beam remains the same as that shown in Fig. 5 for an AOD of thickness L.

Optics EXPRESS

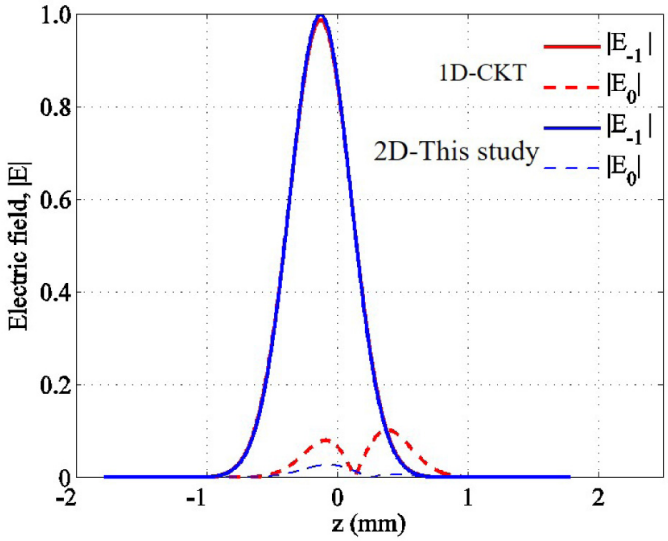

Fig. 6. Magnitude of the electric field (|E|) at the exit boundary for an AOD of thickness 2L, calculated using the Gaussian beam diffraction model of this study and the CKT model for F = 75 MHz, L = 2.24 cm and $\theta_{in} = 0.324^{o}$.

Wang et al. [23] showed that nearly 100% diffraction efficiency can be achieved for a given acoustic beam steering angle, $\tilde{\theta}$ (Fig. 1), by optimizing the acoustic frequency F and the index modulation strength Δn. The steering of acoustic beam produces tilted phase grating inside the AOD device, and the tilt angle automatically modifies the laser incident angle on the grating compared to the original angle of incidence (θ_0) on the AOD device, resulting in a new incident angle $\theta_{in} = \theta_0 + \tilde{\theta}$. So the acoustic frequency and amplitude are modulated to achieve the Bragg diffraction under the new angle of incidence and maximize the diffraction efficiency, respectively. The diffraction efficiency is plotted as a function of the incident angle θ_{in} for different pairs of F and Δn in Fig. 7 for He-Ne lasers, so that each pair has its own Bragg angle of incidence and thus nearly 100% diffraction efficiency is achieved at different values of F. A change in F changes the wavelength, Λ, of the acoustic waves inside the AOD medium and, therefore, the periodicity of the phase grating changes as F is varied. Since the diffraction angle and efficiency depend on the ratio $n_2\lambda_0/\Lambda$, the effect of laser wavelength is examined in Fig. 8 for CO_2 lasers of wavelength 10.6 μm using Ge as the AOD medium. Both Figs. 7 and 8 show that the phased array AODs increase the efficiency and deflection angle. Also the acoustic bandwidth of the AODs increases since nearly 100% diffraction efficiency is achieved over a wide range of acoustic frequency.

Optics EXPRESS

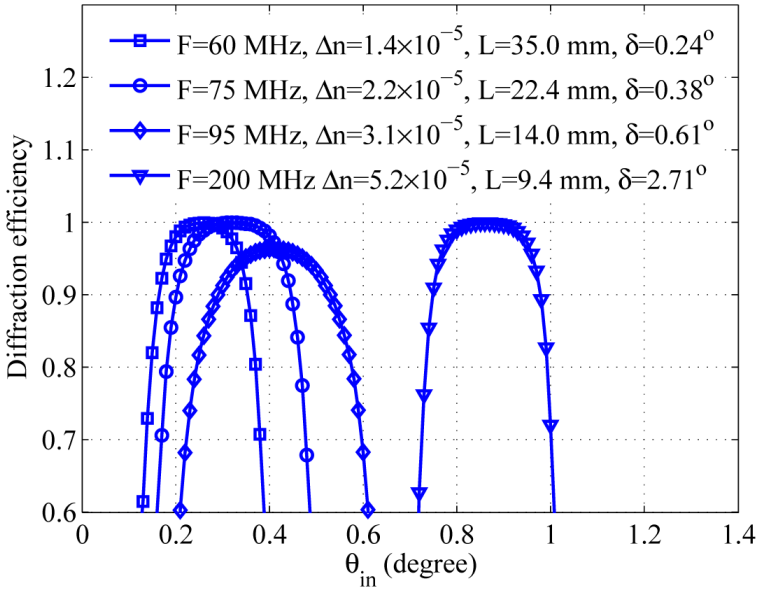

Fig. 7. Diffraction efficiency of TeO_2 ideal AODs as a function of the incident angle θ_{in} for different operating parameters including the phase shift (δ) of acoustic waves between two consecutive transducers.

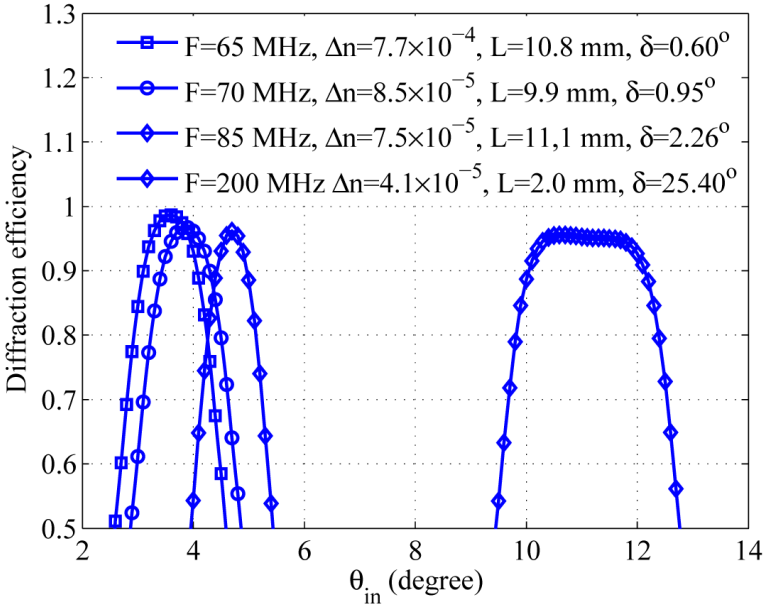

Fig. 8. Diffraction efficiency of Ge ideal AODs as a function of the incident angle θ_{in} for different operating parameters including the phase shift (δ) of acoustic waves between two consecutive transducers.

In Figs. 7 and 8, the acoustic lobes were generated at different steering angles $\tilde{\theta}$ by considering the pitch, i.e., the center-to-center distance between two adjacent transducers, as Λ/2 for each F. Nakahata et al. [24] reported that optimum lobes are produced when the pitch is Λ/2. Since the acoustic lobes affect the shape of the phase grating and Λ depends on F, the pitch was varied for different frequencies to obtain the ideal values of the diffraction

Optics EXPRESS

efficiency and deflection angle under the ideal pitch condition in these two figures. In practice, however, the pitch cannot be varied once the AOD is fabricated with a certain pitch for a given F and, therefore, the diffraction efficiency and deflection angle will deviate from their ideal values. This deviation is studied by determining the real values of the diffraction efficiency and deflection angle for the pitch $\Lambda_m/2$. Here Λ_m is the minimum acoustic wavelength corresponding to the maximum frequency considered in this study for the TeO_2 and Ge AODs. The values of Λ_m are 21 μm and 27.5 μm for the frequency of 200 MHz, based on TeO_2 and Ge respectively. Under this pitch condition, the real values of the diffraction efficiency and deflection angle are compared to their ideal values in Figs. 9 and 10 for the TeO_2 and Ge AODs respectively. Although the real values differ from the ideal values, the maximum deviations of the diffraction efficiency and deflection angle are, respectively, within 32.3% and 0% of the ideal values for the TeO_2 AOD and 76.3% and 0% of the ideal values for the Ge AOD.

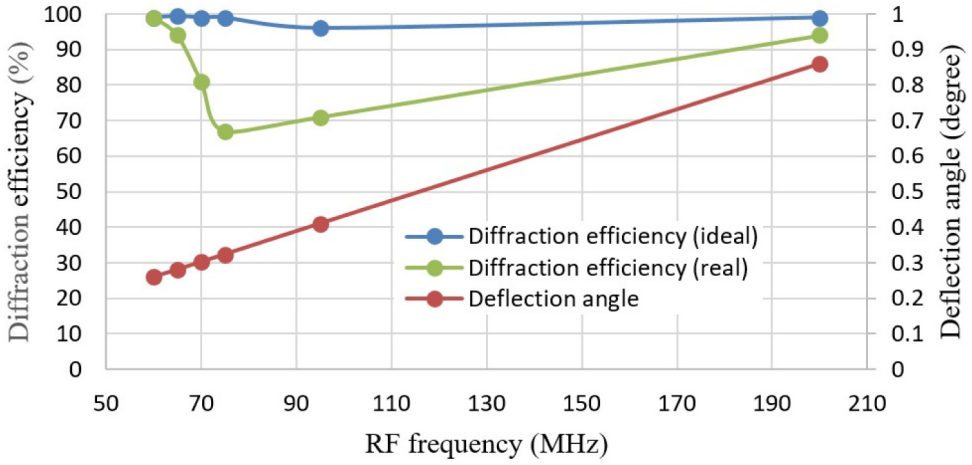

Fig. 9. Comparison between the ideal and real values of the diffraction efficiency and deflection angle for He-Ne lasers and a phased array TeO_2 AOD with pitch S = 10.5 μm for the real AOD.

This reduction in the efficiency is due to the different dimensions of the ideal and real AOD devices. The width and pitch of the transducers and the length of the AOD can be varied arbitrarily in the ideal case to maximize the diffraction efficiency and deflection angle for each acoustic frequency, but the dimensions of the transducers and AOD cannot be altered once an AOD device is fabricated with certain dimensions. Four parameters, which affect the performance of an AOD device, are Δn, L, F and $\tilde{\theta}$. While the acoustic pressure, i.e., the operating radiofrequency power of the transducer, affect Δn, the phase of the acoustic wave at each transducer affect $\tilde{\theta}$. Klein and Cook [33] showed that the laser energy is transferred from the zeroth order mode to the first order diffraction mode and vice versa as a function of L. There is a smallest value of L at which all of the laser energy is transferred to the first order mode to yield 100% diffraction efficiency. As L increases further, the laser energy begins to transfer back to the zeroth order mode from the first order mode to eventually yield 100% energy in the zeroth order mode and 0% diffraction efficiency. With L increasing further, the energy is transferred back to the first order mode, and this energy transfer process between the two modes continues as a function of L. For the real cases of TeO_2 and Ge AODs, the thicknesses of the AOD media are found to be L = 35 mm and L = 11.1 mm, which yield the maximum diffraction efficiency at the radiofrequencies of 65 MHz and 85 MHz respectively. These values of L, however, are not optimum to maximize the performance of the real AOD devices at any other radiofrequencies. This effect of L causes

Optics EXPRESS

incomplete transfer of laser energy from the zeroth order mode to the first-order mode, and thus lowers the diffraction efficiency of real AODs compared to the case of ideal AODs as shown in Figs. 9 and 10.

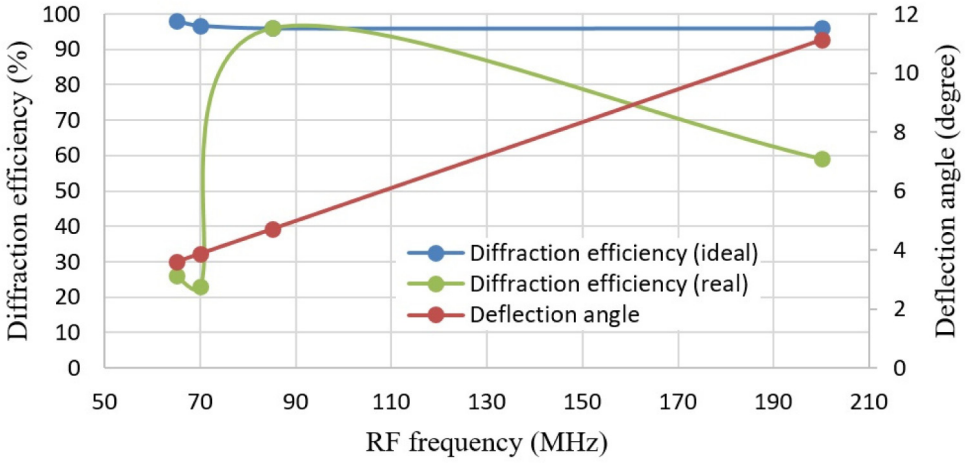

Fig. 10. Comparison between the ideal and real values of the diffraction efficiency and deflection angle for CO_2 lasers and a phased array Ge AOD with pitch S = 13.75 μm for the real AOD.

4. Conclusion

The performance of two phased array AODs is analyzed for Gaussian laser beams of wavelengths 632.8 nm and 10.6 μm by considering two-dimensional refractive index modulation. Nearly 100% diffraction efficiency is achieved without any beam splitting or distortion in the −1 order beam for both two-dimensional and one-dimensional index modulations. The zeroth order beam, however, exhibits less distortion and less electric field in the case of former modulation than the latter. Two-dimensional modulation, therefore, yields slightly higher diffraction efficiency than the one-dimensional modulation. The profile of the distorted beam appears to be non-Gaussian and this profile does not change as the beam propagates outside the AOD medium. The phased array AODs can be operated with nearly 100% diffraction efficiency over a broad range of acoustic frequency and thus the bandwidth of the device increases. Also the acoustic beam steering capability provides a mechanism to create titled phase gratings and this tilt angle can be utilized to achieve large deflection angles for the diffracted laser beam. The theoretical approach of Gaussian beam steering in two-dimensional index dynamic gratings can be applied to predict the performance and technical characteristics of AOD devices, and the results can be used to design AODs for different applications.

Funding

Semiconductor Research Corporation (SRC).

Acknowledgments

This work was supported by SRC and Intel Corporation.